Progress In Electromagnetics Research M, Vol. 81, 85–95, 2019

A Novel Triple Band-Notched UWB Printed Monopole Antenna

Yanming Lv*, Jingjing Zhang, and Huancun Hou

Abstract—A novel ultra-wideband (UWB) printed monopole antenna with triple band-notched characteristics is proposed in this paper. The antenna bandwidth is extended by grooving on the connecting floor and increasing the impedance transformation line, with antenna bandwidth of 3.0∼11 GHz and relative bandwidth of 114%. The overall antenna size is $35 \times 30\,\text{mm}^2$. The complementary split-ring resonators (CSRRs) are loaded on the UWB antenna patch with microstrip wire feed. A symmetric J gap is loaded on the bottom plate, and the spiral gap is loaded on the feeder. The triple band-notched characteristics at 3.22∼3.97 GHz, 4.94∼5.84 GHz, and 7.25∼7.86 GHz bands are realized. The gain of the designed antenna in the notch frequency segment can be reduced rapidly to −4 dbi, while the gain of other frequency bands is above 2 dBi. Simulated and measured results show that the antenna has stable gain and good radiation characteristics in the UWB frequency range.

1. INTRODUCTION

With the continuous advancement of society, people have put forward higher requirements for communication speed and communication effects. Ultra-wideband communication technology meets the pursuit of high-quality communication effects by contemporary people with its advantages of high speed, low power consumption, and high stability. The operating band of a UWB communication system [1] ranges from 3.1 GHz to 10.6 GHz. In this band, there are also downlink band such as WiMAX (3.3∼3.8 GHz), WLAN (5.15∼5.825 GHz), and satellite communication X-band. In order to avoid the interference of these narrow-band systems to UWB system and to meet the needs of miniaturization and integration of the system, the study of notched UWB antennas with band-stop filters has become a hot topic in recent years [2–4].

A more economical and simple method is to structurally modify the UWB antenna to have a high voltage standing wave ratio (VSWR) in a narrow band, while in other bands the VSWR is relatively small, so that it can be filtered. The interference signal in the narrowband communication system is dropped. After a large amount of research, a wide variety of band notch antennas have also appeared in people's field of vision. At present, the commonly used methods to generate notch in the operating frequency of a antenna are grooving, adding open branch, resonator, parasitic unit, and mixing various notch technologies [5–14].

In order to meet the needs of UWB antenna, a UWB antenna with triple band-notched characteristics is presented in this paper. Firstly, a simple microstrip-fed small planar UWB antenna is designed, covering a bandwidth of 3.0–11.6 GHz; secondly, the complementary open resonant ring loaded on the radiation patch can generate notches in the WiMAX band; symmetrical J-shaped slots loaded on the floor can generate notches in WLAN band; the spiral slot loaded on the microstrip line can generate notches for the downlink frequency of X-band. The proposed antenna is simulated and optimized by electromagnetic simulation software HFSS, and the simulation results are further analyzed

Received 22 February 2019, Accepted 30 April 2019, Scheduled 23 May 2019
* Corresponding author: Yanming Lv (yesterday19910@gmail.com).
The authors are with the College of Electronic Information Engineering, Shandong University of Science and Technology, Qingdao, Shandong 266950, China.

and studied. The antenna is manufactured and measured. The results of measurement and simulation are basically the same. It is shown that the antenna has excellent performance and can be applied to a practical UWB system.

2. GEOMETRY OF UWB ANTENNA

The antenna is printed on an FR4 substrate with a dielectric constant of 4.4 and thickness of 1.6 mm. The antenna structure is shown in Figure 1. The dimension of the antenna is $35 \times 30\,\text{mm}^2$. The antenna radiation patch is printed on the front of the dielectric substrate, and the ground plate is printed on the back of the dielectric substrate. The microstrip feeder is fed by a microstrip line. The width of the microstrip feeder is calculated to be 3.07 mm. In order to make the antenna transition smoothly at different resonant frequencies, a 1.3 mm impedance variation line is added between the feeder and the patch, which reduces the sudden change between the feeder and the patch, and expands the antenna bandwidth. At the same time, in order to improve the in-band matching characteristics of the antenna, a rectangular opening of size LC × WC is opened on the ground plate on the back surface of the substrate. Several parameters are optimized in the following discussion using ANSYS HFSS 15.0. Considering the length of the article, we put the simulation optimization curve of LC and WC in the paper. Dimensions of the UWB antenna are listed in Table 1.

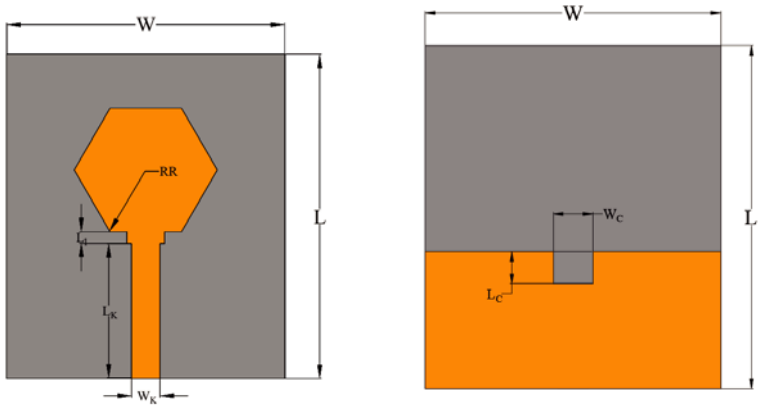

Figure 1. Geometry of the UWB antenna. (a) Top view. (b) Bottom view.

Table 1. Dimensions of the UWB antenna.

Parameter	Value	Parameter	Value
L	35	LC	3.3
W	30	RR	7.7
H	1.6	W1	3.3
L1	1.3	WK	3.07
LK	14.6	WC	4
LD	14		

Figure 2 shows the comparison of the effects of rectangular and non-rectangular slots for S_{11} of the UWB antenna. Figure 2(b) shows the comparison of the return loss measurement results and simulation results of the UWB antenna after optimization. Figure 3 shows the optimized curve of the side lengths LC and WC of the rectangular groove opened on the ground plate on the back side of the substrate.

The fabricated sample of the UWB antenna is shown in Figure 4. The surface current distribution of the UWB antenna is shown in Figure 5. Observing the current distribution on the antenna surface

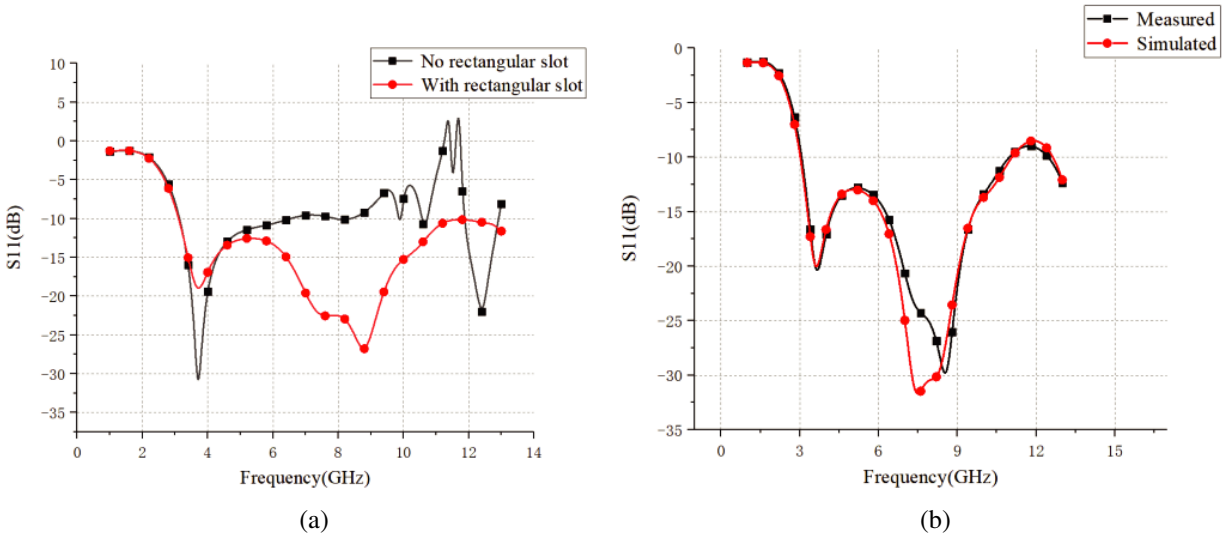

Figure 2. The comparison of results of the UWB antenna. (a) The effect of the rectangular slot for S_{11} of the UWB antenna. (b) Simulated and measured S_{11} of the UWB antenna.

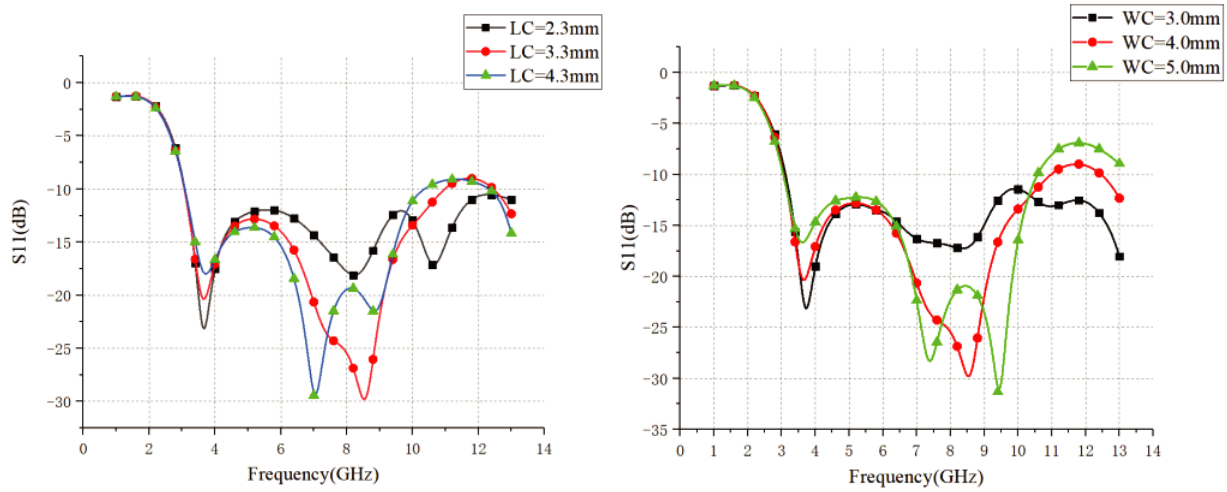

Figure 3. Optimization of rectangular slot dimensions.

allows a more intuitive analysis of the path that produces the resonance, from which the position of the notch structure can be determined.

3. DESIGN OF THE TRIPLE BAND-NOTCHED UWB ANTENNA

In order to reduce the interference between the UWB antenna in the actual communication and the three frequency bands of Wimax, WLAN, and X-band downlink, it is necessary to design an antenna with a three-notch structure to notch the three frequency bands [15]. This dection explains the sequential design techniques in detail, and finally an antenna with triple band-notched characteristics is proposed.

The following empirical formula is used to calculate the total length L of slots in antenna patches:

$$L_{slot} = \frac{c}{2f_{notch}\sqrt{\varepsilon}_{eff}} \tag{1}$$

$$\varepsilon_{eff} = \frac{\varepsilon_r + 1}{2} \tag{2}$$

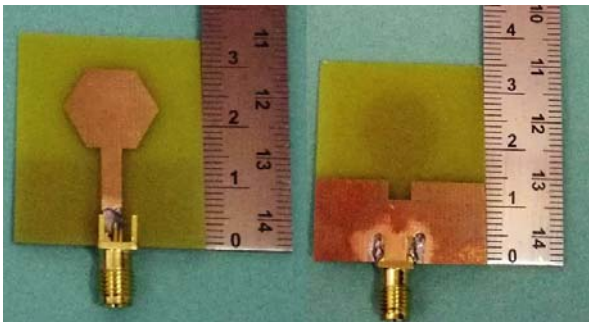

Figure 4. Fabricated sample of the UWB antenna.

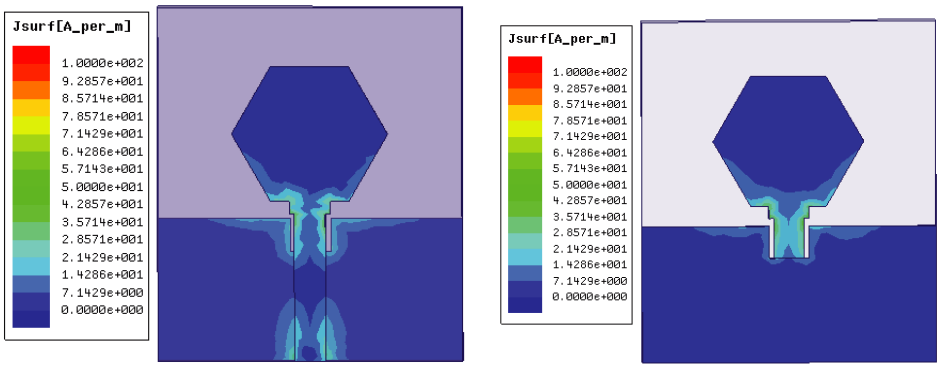

Figure 5. Surface current distribution of the UWB antenna.

where c is the speed of the light in free space, f_{notch} the center frequency of the notch band needed, ε_{eff} the effective dielectric constant of the substrate [16–19], and L the length of the CSRR ring gap. The radius of the ring gap is $R = L_{slot}/2\pi$.

Formula (1) can be used to calculate the initial length of J-shaped slot and spiral slit, and the calculated value $L_J = WJ1 + LJ1 + WJ2 \approx 16.6\,\text{mm}$ and $L_{Spiral} = 2 \times LU + \frac{3}{2}WU + LDDU \approx 12.2\,\text{mm}$.

3.1. Design of the Single Band-Notched UWB Antenna

On the basis of the UWB antenna, the notch of the $3.22 \sim 3.97\,\text{GHz}$ band is realized by loading the CSRR structure on the radiation patch. The CSRR structure can be equivalent to a resonant tank composed of a series of inductors in series [20–24]. The inductor is formed by connecting two half-ring inductors in parallel. In the design of a UWB antenna with notch characteristics, etching the CSRR on the radiating patch is equivalent to introducing a filter at the corresponding frequency, thereby realizing the notch characteristics of the antenna. By observing the current distribution diagram of the UWB antenna, it is determined that the position of the signal radiated by the antenna in the $3.22 \sim 3.97\,\text{GHz}$ band is mainly at the hexagonal radiation patch. Therefore, two concentric rings are embedded on the hexagonal radiation patch to form a CSRR structure. Figure 6 is the structural diagram of the single band-notched antenna. Figure 7 shows the effect of the radius RR1 of the CSRR resonant ring on the single band-notch antenna.

3.2. Design of the Dual Band-Notched UWB Antenna

As shown in Figure 8, the WLAN band notch is achieved by embedding a symmetric J-shaped slot in the ground plane. Since the influences of WJ1 and WJ2 changes on the notch frequency are the same, the influence of parameter WJ2 on the return loss of the antenna is given. The length of the J-shaped

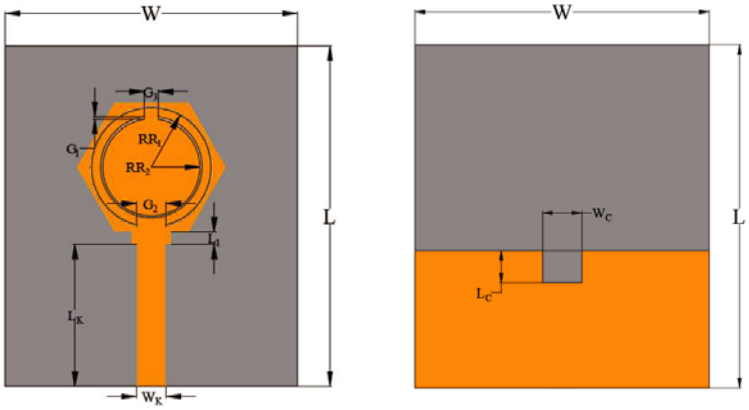

(a) Top view (b) Bottom view

Figure 6. Geometry of the single band-notched UWB antenna.

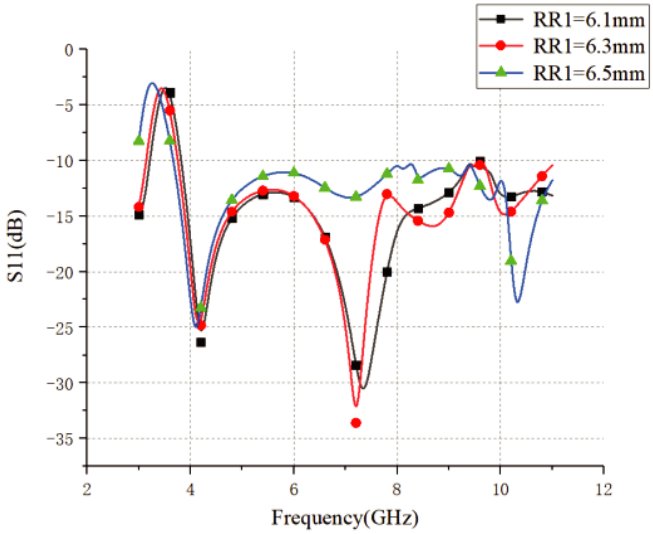

Figure 7. Effect of RR1 on the single band-notched UWB antenna S_{11}.

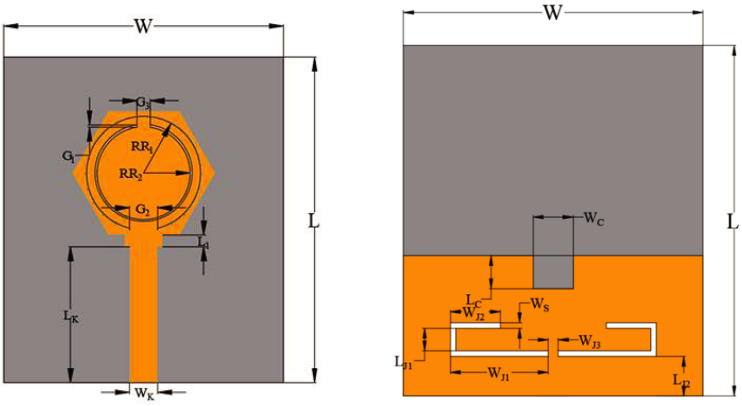

(a) Top view (b) Bottom view

Figure 8. Geometry of the single band-notched UWB antenna.

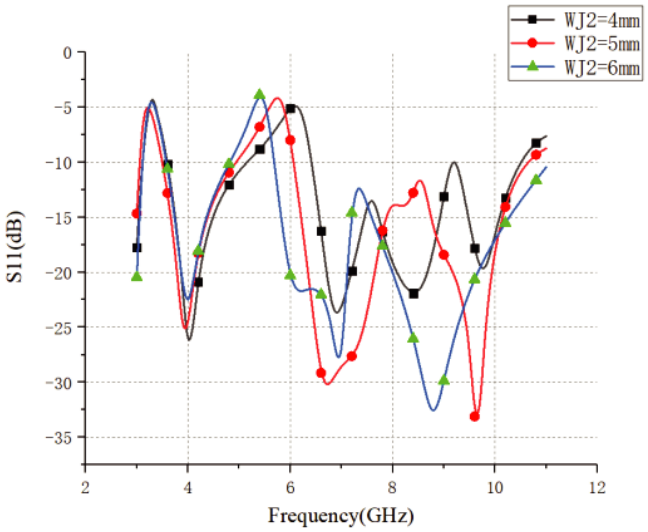

Figure 9. Effect of WJ2 on the dual band-notched UWB antenna S_{11}.

slit is estimated using Equations (1) and (2). As shown in Figure 9, the change in the notch frequency is controlled by changing the length of the J-shaped slit.

3.3. Design of the Triple Band-Notched UWB Antenna

The X-band notch is realized by embedding a spiral gap in the microstrip feeder, and its structure is shown in Figure 10. The length of the spiral gap is estimated using Equations (1) and (2). Figure 11 shows the effect of the parameter LU on the antenna return loss. In this paper, the effect of gradually introducing the resonant element on the return loss to the proposed UWB antenna is shown in Figure 12. Due to the influence of mutual coupling, when the J-shaped slit is embedded in the ground plate, the suppression band of the CSRR is shifted [25–28]. When the spiral slit is embedded in the radiation patch, the suppression band of the CSRR is shifted, but at this time, the suppression band of the J-shaped slit is not significantly affected.

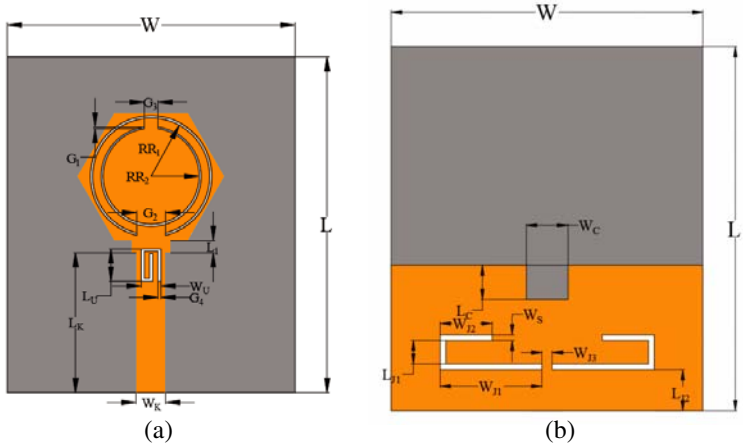

Figure 10. Geometry of the triple band-notched UWB antenna. (a) Top view. (b) Bottom view.

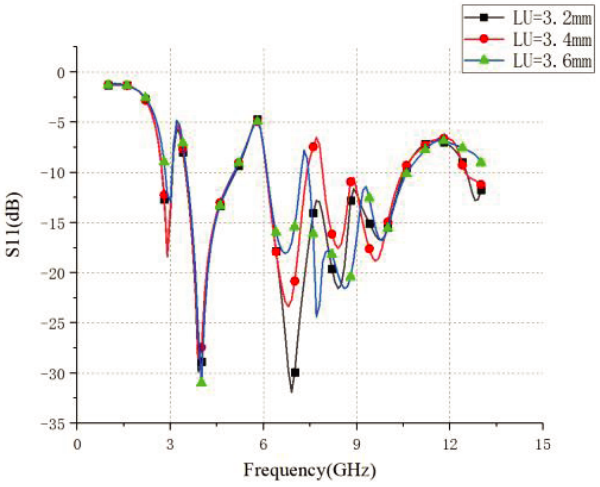

Figure 11. Effect of LU on the triple band-notched UWB antenna S_{11}.

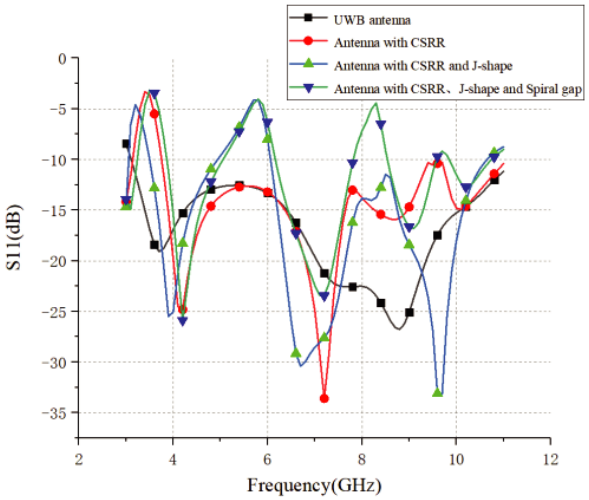

Figure 12. Mutual coupling effect of the notching elements on reflection coefficients.

4. SIMULATED AND MEASURED RESULTS

The specific size and position parameters of CSRR resonant ring, symmetrical J-shaped slot, and spiral slot in the triple band-notched UWB antenna are determined by continuous simulation and analysis with HFSS software. The values of these parameters are given in Table 2.

Table 2. The parameter values of the triple band-notched junction (Units: mm).

Parameter	Value	Parameter	Value
LJ1	2.8	WS	0.55
LJ2	4.5	WU	2
LU	3.4	RR1	6.3
LDU	15	RR2	5
LDDU	2.9	G1	0.5
WJ1	9.8	G2	3
WJ2	5	G3	1.4
WJ3	1	G4	0.3

Figure 13 is the physical picture of the triple band-notched UWB antenna.

Figure 14 shows the comparison between the results of S_{11} measurement and simulation of the triple band-notched UWB antenna. The working bandwidth of the antenna simulation results is 3∼11 GHz, and the notch bands are 3.22∼3.97 GHz, 4.94∼5.84 GHz, and 7.25∼7.86 GHz, respectively. The measurement results of the antenna are in good agreement with the simulation ones. The deviation is due to processing errors, and SMA joint welding will lead to changes in test results. Figure 15 shows the comparison between the VSWR test results and simulation results of the triple band-notched UWB antenna.

The triple band-notched UWB antenna pattern also selects the frequency corresponding to the lowest value of the return loss as the observation frequency. Figure 15 shows the radiation patterns of the E-plane and H-plane of the triple band-notched UWB antenna at 4.5 GHz, 6.5 GHz, and 9.5 GHz. It can be seen from Figure 16 that the radiation pattern of the E plane of the antenna is similar to the "8" shape, and the H-plane radiation pattern indicates that the antenna has an

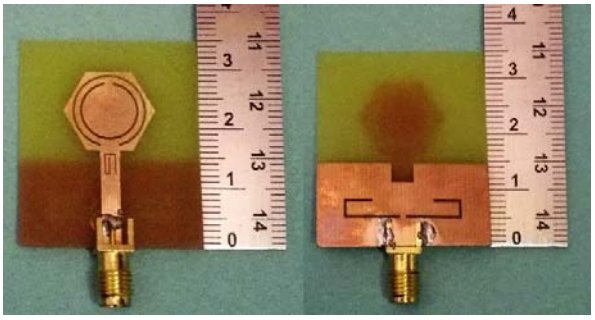

Figure 13. Photograph of the triple band-notched UWB antenna.

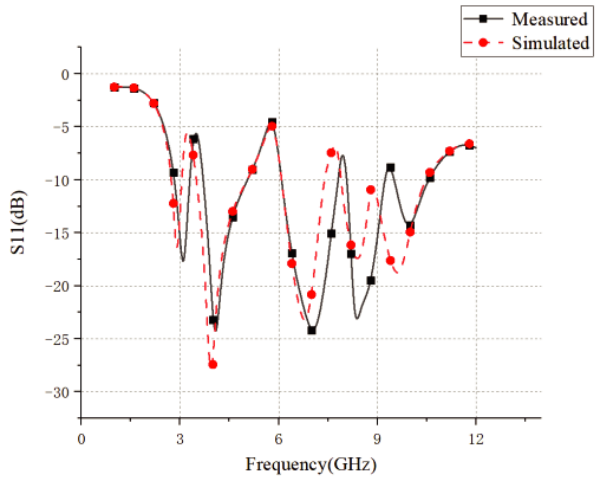

Figure 14. Simulated and measured S_{11} of the proposed antenna.

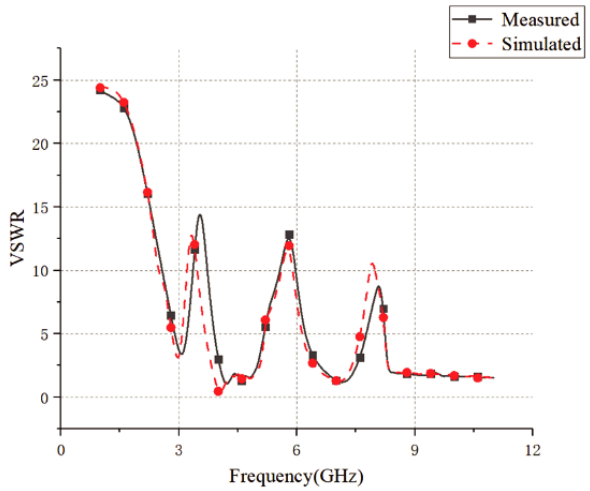

Figure 15. Simulated and measured VSWR of the proposed antenna.

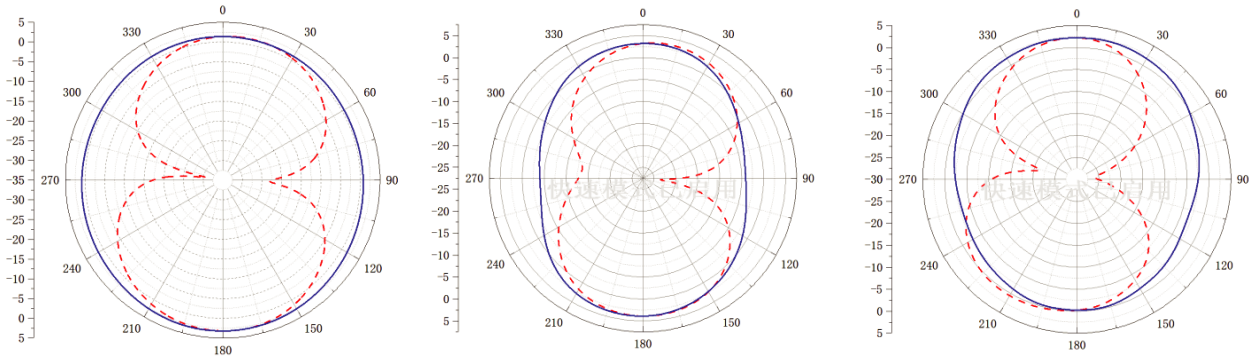

(a) 4.5GHz (b) 6.5GHz (c) 9.5GHz

Figure 16. Radiation pattern of the triple band-notched UWB antenna.

approximately omnidirectional radiation characteristic, so the antenna has good radiation characteristics at the operating frequency band. Figure 17 shows the surface current distribution of the triple band-notched UWB antenna at 3.5 GHz, 5.5 GHz, and 7.5 GHz, respectively.

Figure 18 shows the simulated gain of the proposed triple band-notched antenna. The maximum

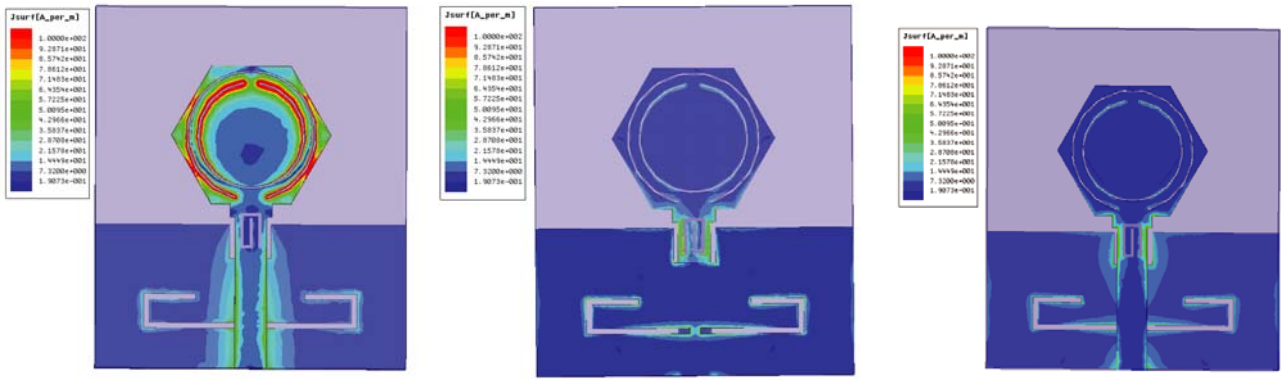

(a) (b) (c)

Figure 17. Surface current distribution of the triple band-notched UWB antenna.

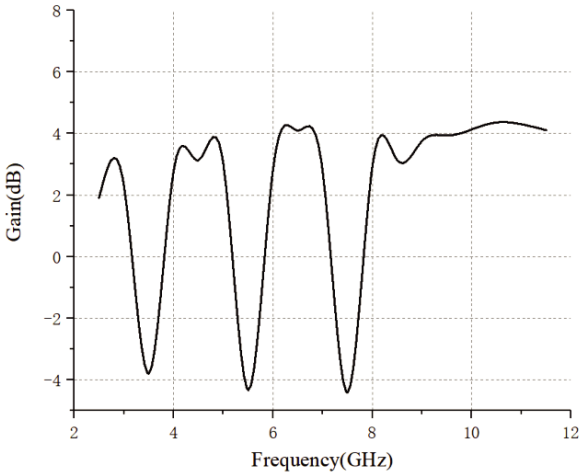

Figure 18. The simulated gain of the triple bandnotched UWB antenna.

gain of the antenna in the non-notch band is 4.3 dB, and the minimum gain is 2 dB. The gain is less than 0 dB in the three notch bands, and the lowest is around −4 dB. In general, the antenna has a relatively stable gain over the entire operating frequency band, and the gain rapidly drops below 0 dB in the three notch bands. It indicates that the designed triple band-notched antenna can work in the UWB frequency range and can filter out WiMAX bands, WLAN bands, and Satellite communication X-band downlink frequency segment.

5. CONCLUSION

This paper proposes a triple band-notched UWB printed monopole antenna with a antenna bandwidth of 3.0 to 11 GHz and relative bandwidth of 114%. Triple band-notched characteristics at 3.22 ∼3.97 GHz, 4.94∼5.84 GHz, and 7.25∼7.86 GHz bands are obtained by etching the CSRR resonant ring on the radiation patch, etching the symmetric J-shaped slot on the floor, and etching the spiral slot on the feeding line. The antenna can effectively filter out WiMAX (3.3∼3.8 GHz), WLAN (5.15∼5.825 GHz), and satellite communication system X-band downlink frequency segment (7.25∼7.75 GHz). The antenna's radiation characteristics and gains have also been examined. Moreover, the antenna is expected to get applications in various UWB systems.

REFERENCES

1. Chen, D. and C.-H. Cheng, "A novel compact ultra-wideband (UWB) wide slot antenna with via holes," *Progress In Electromagnetics Research*, Vol. 94, 343–349, 2009.
2. Lee, J. N. and J. K. Park, "Compact UWB chip antenna design using the coupling concept," *Progress In Electromagnetics Research*, Vol. 90, 341–351, 2009.
3. Lin, S., S. Yang, A. E. Fathy, and A. Elsherbini, "Development of a novel UWB vivaldi antenna array using SIW technology," *Progress In Electromagnetics Research*, Vol. 90, 369–384, 2009.
4. Lin, C.-C. and H.-R. Chuang, "A 3–12 GHz UWB planar triangular monopole antenna with ridged ground-plane," *Progress In Electromagnetics Research*, Vol. 83, 307–321, 2008.
5. Fallahi, R., A. A. Kalteh, and M. G. Roozbahani, "A novel UWB elliptical slot antenna with band-notched characteristics," *Progress In Electromagnetics Research*, Vol. 82, 127–136, 2008.
6. Yang, Y., Y. Wang, and A. E. Fathy, "Design of compact vivaldi antenna arrays for UWB see through wall applications," *Progress In Electromagnetics Research*, Vol. 82, 401–418, 2008.
7. Akhoondzadeh-Asl, L., M. Fardis, A. Abolghasemi, and G. R. Dadashzadeh, "Frequency and time domain characteristic of a novel notch frequency UWB antenna," *Progress In Electromagnetics Research*, Vol. 80, 337–348, 2008.
8. Dehdasht-Heydari, R., H. R. Hassani, and A. R. R. Mallahzadeh, "Quad ridged horn antenna for UWB applications," *Progress In Electromagnetics Research*, Vol. 79, 23–38, 2008.
9. Raad, H. K., "An UWB antenna array for flexible IoT wireless systems," *Progress In Electromagnetics Research*, Vol. 162, 109–121, 2018.
10. Ma, K., Z. Zhao, J. Wu, S. M. Ellis, and Z.-P. Nie, "A printed Vivaldi antenna with improved radiation patterns by using two pairs of eye-shaped slots for UWB applications," *Progress In Electromagnetics Research*, Vol. 148, 63–71, 2014.
11. Samal, P. B., P. J. Soh, and G. A. E. Vandenbosch, "A systematic design procedure for microstrip-based unidirectional UWB antennas," *Progress In Electromagnetics Research*, Vol. 143, 105–130, 2013.
12. Wu, Z. H., F. Wei, X.-W. Shi, and W.-T. Li, "A compact quad band-notched UWB monopole antenna loaded one lateral L-shaped slot," *Progress In Electromagnetics Research*, Vol. 139, 303–315, 2013.
13. Li, G., H. Zhai, T. Li, X. Y. Ma, and C.-H. Liang, "Design of a compact UWB antenna integrated with GSM/Wcdma/WLAN bands," *Progress In Electromagnetics Research*, Vol. 136, 409–419, 2013.
14. Liu, X. L., Y.-Z. Yin, P. A. Liu, J. H. Wang, and B. Xu, "A CPW-fed dual band-notched UWB antenna with a pair of bended dual-L-shape parasitic branches," *Progress In Electromagnetics Research*, Vol. 136, 623–634, 2013.
15. Islam, M. T., R. Azim, and A. T. Mobashsher, "Triple band-notched planar UWB antenna using parasitic strips," *Progress In Electromagnetics Research*, Vol. 129, 161–179, 2012.
16. Awais, Q, H. Tariq Chattha, M. Jamil, Y. Jin, F. A. Tahir, and M. Ur Rehman, "A novel dual ultrawideband CPW-fed printed antenna for Internet of Things (IoT) applications," *Wireless Communications and Mobile Computing*, Vol. 10, 1–9, 2018.
17. Ren, J., D. Mi, and Y. Yin, "Compact ultrawideband MIMO antenna with WLAN/UWB bands coverage," *Progress In Electromagnetics Research C*, Vol. 50, 121–129, 2014.
18. Saleem, R. and A. K. Brown, "Empirical miniaturization analysis of inverse parabolic step sequence based UWB antennas," *Progress In Electromagnetics Research*, Vol. 114, 369–381, 2011.
19. Thomas, K. G. and M. Sreenivasan, "A simple ultrawideband planar rectangular printed antenna with band dispensation," *IEEE Trans. on Antennas and Propag.*, Vol. 58, No. 1, 27–34, Jan. 2010.
20. Abdollahvand, M., G. Dadashzadeh, and D. Mostafa, "Compact dual band-notched printed monopole antenna for UWB application," *IEEE Antennas Wireless Propag. Lett.*, Vol. 9, 1148–1151, 2010.

21. Trang, N. D, D. H. Lee, and H. C. Park, "Design and analysis of compact printed triple band-notched UWB antenna," *IEEE Antennas Wireless Propag. Lett.*, Vol. 10, 403–406, 2011.
22. Sim, C.-Y.-D., W.-T. Chung, and C.-H. Lee, "Planar UWB antenna with 5 GHz band rejection switching function at ground plane," *Progress In Electromagnetics Research*, Vol. 106, 321–333, 2009.
23. Haroon, S., K. S. Alimgeer, N. Khalid, et al., "A low profile UWB antenna with triple band suppression characteristics," *Wireless Personal Communications*, Vol. 82, No. 1, 495–507, May 2015.
24. Taha-Ahmed, B. and E. M. Lasa "Polarization diversity UWB antennas with and without notched bands," *Progress In Electromagnetics Research M*, Vol. 76, 101–111, 2018.
25. Shi, M., L. Cui, H. Liu, M. Lv, and X.-B. Sun "A new UWB antenna with band-notched characteristic," *Progress In Electromagnetics Research M*, Vol. 74, 201–209, 2018.
26. Ebrahimi, A. and H. Khodabakhshi,"Design of a novel UWB microstrip antenna with SIW feed," *Progress In Electromagnetics Research M*, Vol. 64, 87–97, 2018.
27. Yadav, D., M. P. Abegaonkar, S. K. Koul, V. N. Tiwari, and D. Bhatnagar "Two element band-notched UWB MIMO antenna with high and uniform isolation," *Progress In Electromagnetics Research M*, Vol. 63, 119–129, 2018.
28. Li, J.-F., D.-L. Wu, and Y.-J. Wu, "Dual band-notched UWB MIMO antenna with uniform rejection performance," *Progress In Electromagnetics Research M*, Vol. 54, 103–111, 2017.